Journal of Chromatography A, 1217 (2010) 7255–7264

Contents lists available at ScienceDirect

Journal of Chromatography A

journal homepage: www.elsevier.com/locate/chroma

Separation of triphenyl atropisomers of a pharmaceutical compound on a novel mixed mode stationary phase: A case study involving dynamic chromatography, dynamic NMR and molecular modeling

X. Bu[a], P.J. Skrdla[b], P.G. Dormer[c], Y. Bereznitski[a,*]

[a] Early Development Analytical Research, Merck, Sharp and Dohme, Rahway, NJ 07065, USA
[b] Global Pharmaceutical Commercialization, Merck, Sharp and Dohme, Rahway, NJ 07065, USA
[c] Process Research, Merck, Sharp and Dohme, Rahway, NJ 07065, USA

ARTICLE INFO

Article history:
Received 15 June 2010
Received in revised form 9 September 2010
Accepted 14 September 2010
Available online 19 September 2010

Keywords:
Dynamic HPLC
NMR
Atropisomer separation
Molecular modeling
Interconversion kinetics

ABSTRACT

Analysis of atropisomers is of considerable interest in the pharmaceutical industry. For complex chiral molecules with several chiral centers hindered axial rotation can lead to formation of interconverting diastereomers that should be separable on achiral stationary phases. However, achieving the actual separation may be difficult as the on-column separation speed must match or be faster then the rate of isomer interconversion. Often, this requirement can be satisfied by using low-temperature conditions and by improving selectivity via use of chiral stationary phases. In the current study, we present an alternative approach utilizing an Obelisc R column, a novel mixed mode stationary phase that provided acceptable separation of triphenyl atropisomers inside a conventional HPLC temperature range. The separation was investigated under various chromatographic conditions. The interconversion chromatograms exhibited classic peak–plateau-peak behavior indicating the simultaneous atropisomer separation and interconversion. The elution profiles were integrated in order to deconvolute the peak areas of the "pure" (non-exchanged) and interconverted species; these data were used to obtain kinetic information. Analysis of retention data rendered thermodynamic information on the mechanism of retention and selectivity. Chromatographic kinetic data were complemented with variable-temperature NMR and molecular modeling studies, which provided additional support and insights into the energetics of the interconversion process.

1. Introduction

Studies of atropisomerism have been a subject of enduring interest among scientists in academia and industry. From a pharmaceutical perspective, fundamental knowledge of axial chirality and stereo-dynamics is important for design of new molecular entities, enhanced understanding of structure–property relationships, and control of isomeric impurities. Analysis of atropisomers receives significant attention during pharmaceutical development due to potential implications arising from differences in their physicochemical properties, bioavailability, and clinical safety (pharmacokinetics, pharmacodynamics, and toxicological activity). Although interconversion of stereo-labile compounds can be studied by variety of dynamic (such as planar chromatography, CE, SFC, CEC, MEKC, GC, etc.) [1–5] and stop-flow methods [6], dynamic NMR and HPLC are likely the most commonly used due to widespread popularity of these techniques, and their orthogonal nature [7–10]. Dynamic HPLC (DHPLC) is especially useful for kinetic studies of systems with slow internal motion. The time scale of this technique extends from seconds to hours. DHPLC typically encompasses dynamic processes with activation energy in the range of 70–120 kJ/mol [11]. Although dynamic HPLC is considered to be complementary method to dynamic NMR (where kinetic parameters can be measured directly), dynamic HPLC has a number of important advantages, such as low quantity of material needed for measurements, ability to employ wide range of non-deuterated solvents and experimental conditions, and a possibility of physical isolation of isomers for further characterization. This technique is also less expensive and more readily available.

A key precondition for successful dynamic chromatography experiments is separability of the interconverting isomers. For complex pharmaceutical molecules with multiple chiral centers, hindered axial rotation will lead to formation of configurational isomers (diastereomers of each other), which should be amenable to chromatographic separation on achiral stationary phases. However, the liquid chromatographic separation of iso-

* Corresponding author at: Early Development Analytical Research, Merck, Sharp and Dohme, POB 2000, RY818-B221, Rahway, NJ 07065, USA. Tel.: +1 732 594 0486; fax: +1 732 594 3887.
E-mail address: yuri_bereznitski@merck.com (Y. Bereznitski).

0021-9673/$ – see front matter © 2010 Elsevier B.V. All rights reserved.
doi:10.1016/j.chroma.2010.09.042

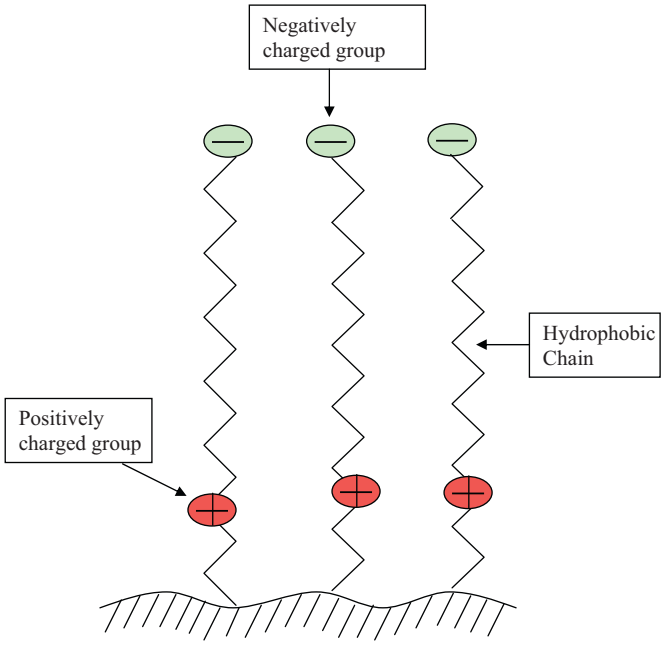

Fig. 1. Schematic representation of the Obelisc R phase. Exact chemistry of the phase was not disclosed, the structure shown here was reproduced after illustrations provided by supplier.

mers with axial chirality can be difficult on conventional (alkyl type) chromatographic phases as the separation speed (rate of molecular partitioning process between mobile and stationary phases) must match, or be faster than the rate of the isomer interconversion. Often, these requirements can be satisfied by using low-temperature (even cryogenic) chromatographic conditions and by introducing additional selectivity employing chiral stationary phases (CSPs) [12,13].

Lower temperatures typically will slow down the rate of interconversion by reducing the average molecular kinetic energy. On the other hand, the use of chiral phases will expose atropisomers to various interaction sites, which can affect the ability of the analytes to interconvert [12]. Often, the former effect can be offset by sharp decrease in chromatographic efficiency as a result of rapidly growing mobile phase viscosity at lower temperatures. As for the latter, interaction sites of the CSP (both enantio-selective and non-specific) may not always have a desired effect on atropisomer interactions to significantly affect the rate of isomer separation, and improve selectivity.

In the current work the authors discuss atropisomer separation approach using Obelisc R column, a novel stationary phase developed by SIELC Technologies [14]. This phase is synthesized employing proprietary chemical modification technology that supposedly creates a unique separation environment with its own charge characteristics, ionic strength, and hydrophobic properties. The Obelisc R ligand contains negatively and positively charged groups separated by a long hydrophobic linkage. The negatively charged group is located at the terminal position, while positively charged group is on the opposite end of the hydrophobic chain close to the silica gel surface (see Fig. 1). The vendor claims that the internal environment of the phase contains both stationary (bound) and exchangeable (mobile phase) components. Furthermore, the ionic strength in the pores is estimated to be significantly higher then ionic strength in the mobile phase [15]. On the other hand, both the positive and negative charges of the ligands can simultaneously participate in electrostatic interactions. The combination of these attributes makes Obelisc R phase a potentially valuable tool for complex analytical separations.

Despite promising set of separation features and tunable properties, this mixed mode phase has been sparsely characterized in the scientific literature [16]. The current study attempted to address some of these deficiencies by undertaking investigation of atropisomer separation. The separation was investigated under various chromatographic conditions, including variable temperature, pH, flow rate and ionic strength. Analysis of chromatographic data rendered kinetic and thermodynamic information on the atropisomer separation process. The dynamic chromatography data were complemented with information from variable-temperature NMR studies and molecular modeling simulations, which provided additional support and insights into the energetics of the interconversion process.

2. Experimental

2.1. Chemicals

HPLC-grade acetonitrile, methanol, and phosphoric acid (85%) were purchased from Sigma–Aldrich (St. Louis, MO, USA). Potassium phosphate monobasic and Dibasic (KH_2PO_4 and K_2HPO_4) buffer salts were from J.T. Baker (Phillipsburg, NJ, USA). High-purity water, 18.2 MΩ, obtained from a HYDRO System (Garfield, NJ, USA) was used to prepare all the aqueous mobile phases and phosphate buffer solutions. Phosphoric acid was used for pH adjustment of the aqueous buffers. The triphenyl pharmaceutical intermediate used in this study was produced at Merck Process Research (Rahway, NJ). The analyte samples were dissolved in 50/50 water–acetonitrile, at a concentration of 0.5 mg/mL.

2.2. HPLC conditions

Separation of the pharmaceutical triphenyl atropisomers was carried out with an Agilent 1100 HPLC system (Santa Clara, CA, USA), comprising an autosampler, high-pressure binary pump, heated column thermostat and variable wavelength UV detector set to a wavelength of 210 nm. Chromatographic system was equipped with 4.6 × 150 mm, 5 μm particle size Obelisc R column purchased from SIELC Technologies (Prospect Heights, IL USA). During dynamic chromatography experiments the column temperature varied from 5 to 50 °C, and flow rate varied from 0.5 to 1.8 mL/min. The injection volume was 5 μL. Mobile Phase A was 0.1 vol.% H_3PO_4 in water or other phosphate aqueous buffers, and B was 100% acetonitrile. Dynamic HPLC chromatograms were obtained under isocratic condition with 40 vol.% organic mobile phase. The column was conditioned at the respective conditions prior to analysis, and multiple injections were made at each condition to ensure reproducibility.

LC–MS analysis was performed using Agilent 1100 HPLC system equipped with Agilent 6300 Series Ion Trap LC/MS detector. In that case, trifluoroacetic acid was used as a suitable aqueous mobile phase modifier in place of the phosphate buffer.

2.3. Variable temperature NMR experiments

^{1}H NMR spectra were recorded on 500 MHz Bruker Avance AV III spectrometer equipped with variable temperature probe. Chemical shifts were quoted in ppm relative to tetramethylsilane. Probe temperature was calibrated using proton frequency difference of the methylene and hydroxyl peaks of neat ethylene glycol (273–416 K range).

2.4. Theoretical calculations

Molecular modeling studies were conducted using Spartan'08, a computational package developed by Wavefunction, Inc. (Irvine,

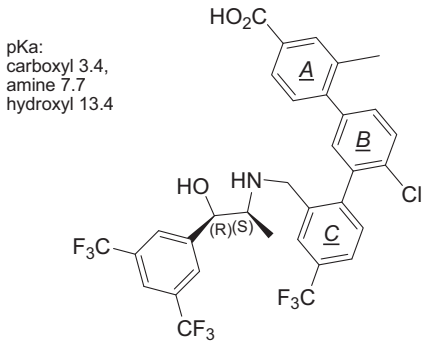

Fig. 2. Structure of the triphenyl intermediate. Acid dissociation constants (pK_a) are estimates obtained using ACD Labs software. Note the triphenyl rings were labeled as *A*, *B*, and *C* to facilitate discussion in the text.

CA, USA). The lowest energy conformer structure was obtained using energy minimization procedure employed to locate global minimum. The transition state species was modeled as the highest-energy configuration that could be obtained via rotation of a single bond connecting respective phenyl rings. A potential energy function for rotational conformers was generated using molecular mechanics (MMFF) method, further refinement was performed using Hartree-Fock (HF) method.

In order to rationalize interactions of analyte with the stationary phase, an estimate of acid ionization constants (pK_a) for the analyte was obtained using ACD Labs PhysChem Suite software version 11.02 (Toronto, ON, Canada).

3. Results and discussion

The analyte of interest in this work is an triphenyl intermediate (TP). It is a critical precursor in the synthesis of a novel cholesteryl esterase transfer protein inhibitor (CETP) drug. Molecular structure of this intermediate is shown in Fig. 2. The TP molecule contains two chiral centers. Additionally, it contains a terminal fragment with three consecutive aryl groups containing different *ortho* substituents. These structural features are characteristic of a molecule with the potential for hindered rotation about the single bonds connecting the aryl groups, which can lead to formation of configurational isomers (atropisomers); in this case, they are diastereomers of each other. In order to establish stereodynamic control, chromatographic separation of triphenyl configurational isomers was attempted using several conventional, commercially available reversed phase stationary phases such as octyl, and octadecyl alkyl phases as well as phases with embedded polar groups (amide, ether link). Additionally, phases with phenyl and pentafluorophenyl groups were evaluated. However, none of the above-mentioned phases was successful in separating the triphenyl atropisomers.

A typical chromatogram obtained for triphenyl analysis using octyl phase is shown in Fig. 3a. As can be seen, a single peak appears to be noticeably broadened, which may serve as an indication of the unresolved atropisomers' presence. This effect is unlikely to be caused by chromatographic artifact (e.g. solvent mismatch), as the analyte was dissolved in a diluent matching the composition of the eluent mobile phase. Similar peak broadening effects were observed for the other columns used in the column screening study. On the other hand, a successful separation of triphenyl isomers was achieved using the SIELC Obelisc R column (Fig. 3b). However, triphenyl injection resulted in a classic peak–plateau-peak shape characteristic of simultaneous on-column separation and interconversion (i.e. dynamic chromatograms). Confirmation of the interconversion process was obtained using LC-MS, which identified the presence of molecular ions consistent with the triphenyl mass-to-charge ratio throughout the entire interconversion region.

In order to gain mechanistic understanding of the separation process, further investigation was focused on examining the role of adjustable chromatographic parameters on isomer retention and interconversion. The following subsections will examine the influence of temperature, pH, flow rate and ionic strength on separation of the TP atropisomers as well as investigate the kinetic and energetic aspects of the atropisomer interconversion.

3.1. Temperature, flow rate, pH and ionic strength study effect on separation

As mentioned above, separation of triphenyl rotamers can be accomplished on SIELC Obelisc R column using 0.1 vol.% H_3PO_4 – acetonitrile mobile phase (60/40, v/v). Fig. 4 illustrates the influence of temperature variation on the chromatographic separation. As can be noted at 5 °C, the diastereomeric atropisomers are essentially baseline separated. The injection results in two distinct chromatographic peaks which correspond to "pure" (unconverted)

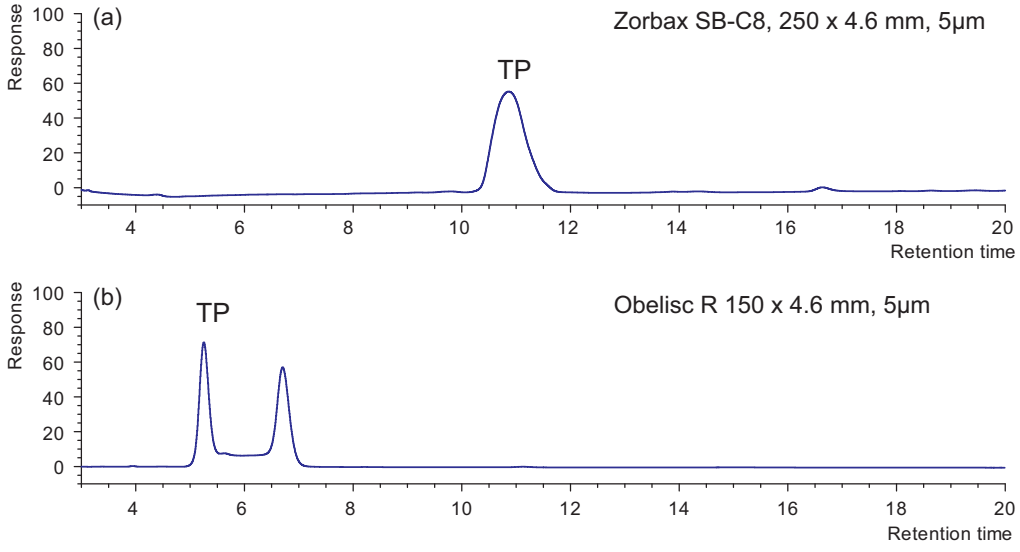

Fig. 3. Analysis of triphenyl on Zorbax SB-C8 and Obelisc R columns. For either column mobile phase was water (0.1 vol.% H_3PO_4)–acetonitrile (60/40, v/v), column temperature 25 °C, and flow rate 1.0 mL/min. UV detection at 210 nm.

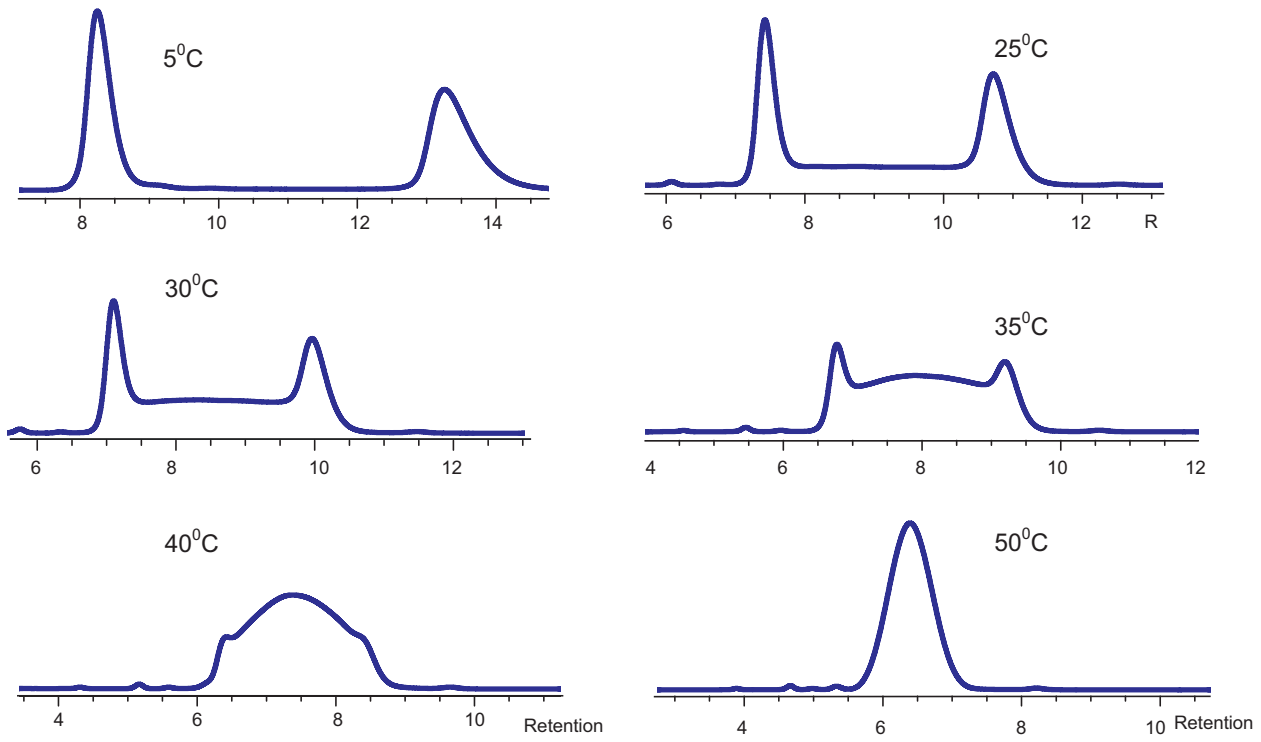

Fig. 4. Influence of temperature on the on-column interconversion of triphenyl atropisomers. Chromatographic conditions: Obelisc R (4.6 × 150 mm), water (0.1 vol.% H_3PO_4)–acetonitrile (60/40, v/v) mobile phase, flow rate 1.0 mL/min. UV detection at 210 nm.

isomers. Absence of the plateau between these peaks serves as an indication that no significant interconversion is evident at this temperature. When the temperature is increased, the increased kinetic energy of the analyte molecules results in weaker interaction with the stationary phase, and chromatographic retention decreases. By the same token, as more energy is supplied to the system, the configurational isomers begin to interconvert at a faster rate. This is evidenced by rising plateau connecting the two peaks of "pure" isomers. The plateau consists of molecules that interconverted at least once on-column, prior to reaching detector. The observed temperature dependent plateaus between two "pure" peaks at elevated temperatures are a result of simultaneous interconversion and separation. At the temperatures above 35 °C increasing internal energy produces faster interconversion, and the "pure" peaks of isomers begin to effectively disappear. This effect leads to a single peak at 50 °C (i.e. peak coalescence). At this temperature interconversion rate is faster then the HPLC time scale of separation (i.e. rate of partitioning), which results in peak coalescence. Overall, the temperature studies reflect range showing transition from a slow to fast exchange between the interconverting species.

Fig. 5 shows influence of mobile phase pH changes on elution profile of triphenyl atropisomers. Experiments were conducted at a constant temperature of 25 °C using 0.1 vol.% phosphoric acid in water–acetonitrile mobile phase (60:40, v/v). For each set of experiments acidity of the aqueous phase buffer was adjusted to achieve different pH values. After each pH change the chromatographic system was allowed to re-equilibrate for at least two hours to achieve reproducible elution profiles. As can be inferred from chromatograms produced by these experiments, the effect of increasing pH appears to be qualitatively similar to that of rising temperature with the exception of its influence on retention times. As Fig. 5 shows, increase in pH results in decrease of the areas of "pure" components accompanied by concurrent increase of interconversion (plateau) area. At pH = 2.75 pure components represent significantly less then half of the total area under the curve, and at pH = 3.0 all triphenyl molecules are involved in on-column interconversion.

This phenomenon can be rationalized if the molecular structures of the analyte and Obelisc R ligand are taken into consideration. It can be seen from Fig. 2, the analyte molecule contains carboxyl and amino groups. Their estimated pK_a values are 3.4 and 7.7, respectively. Hence, at pH = 2.0 the amine site of the analyte will be protonated, and the dissociation of triphenyl carboxyl group will be significantly suppressed. On the other hand, the Obelisc R ligands contain positively charged (quarternary amine like) and negatively charged (carboxyl type) fragments in the structure. The pK_a values estimated by SIELC are 10.0 and 4.0 for the amine and carboxyl sites, respectively [15]. Thus, at pH = 2.0 dissociation of the carboxyl group will be insignificant, while amine site of the ligand will be fully charged. As the mobile phase pH increases, dissociation of carboxyl groups of the ligand and especially those of triphenyl molecules becomes more pronounced, leading to increased ionic interactions between analyte molecules and the stationary phase. This results in increased analyte retention, and consequently, decreased speed of separation. Thus, slowing down the rate of separation results in an increased amount of interconverted molecules manifested as a growing interconversion region (plateau area). Longer time on the column leads to increased amount of interconversion (at fixed column temperature).

A somewhat similar trend was observed for separations performed at variable flow rates at constant temperature. Fig. 6 shows elution profiles of triphenyl rotamers obtained using the same method at 25 °C with 0.1 vol.% phosphoric acid in water–acetonitrile (60:40, v/v) mobile phase with variable flow rates. The flow rate values in these experiments were varied between 0.5 and 1.8 mL/min. Deconvolution of the peak areas corresponding to "pure" components indicated that relative contribution of the "pure" (unconverted) components to the total area steadily decreased with decreasing flow rate, demonstrating that longer separation time leads to increased on-column interconversion (growing plateau area), as expected.

Finally, Fig. 7 demonstrates the effect of the buffer concentration on the on-column interconversion of triphenyl isomers. As can

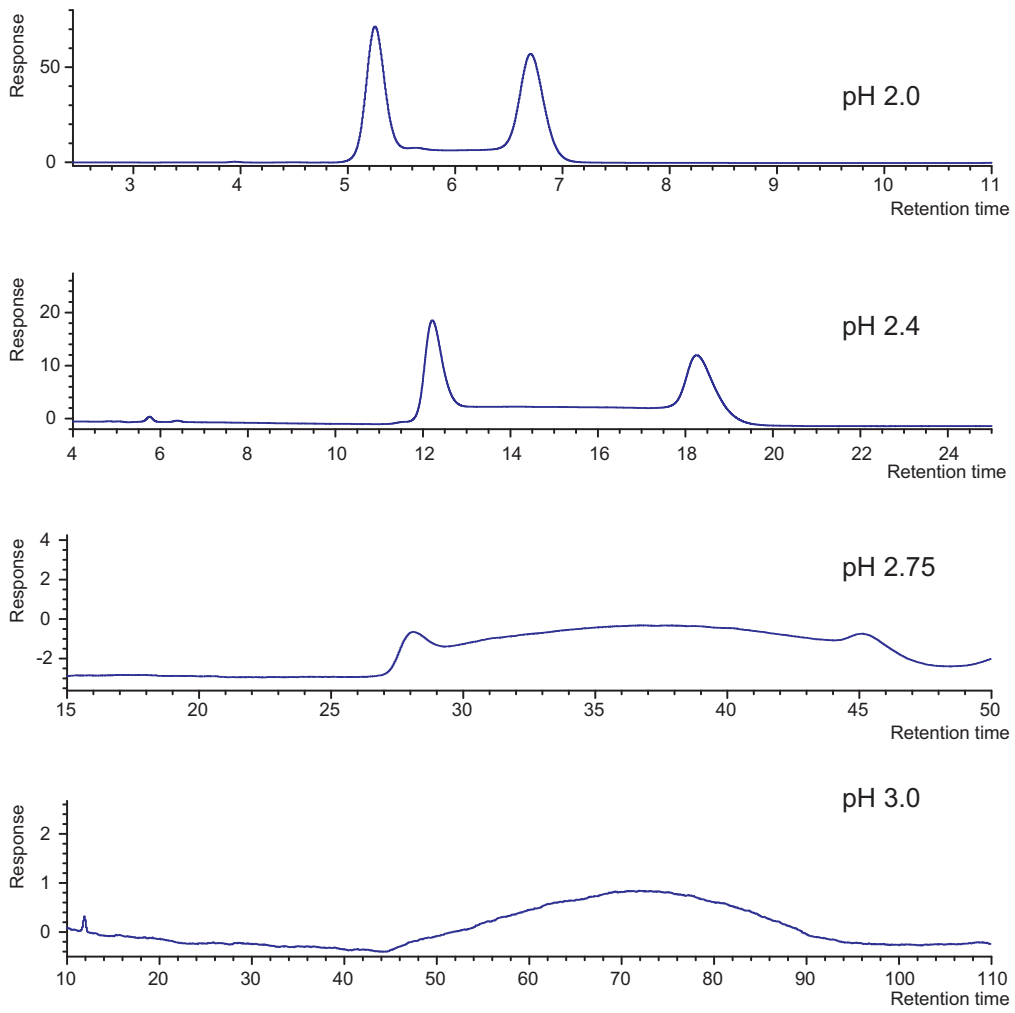

Fig. 5. Influence of mobile phase pH on the on-column interconversion of triphenyl atropisomers. Chromatographic conditions: Obelisc R (4.6 × 150 mm), water (phosphate buffer)–acetonitrile (60/40, v/v) mobile phase, column temperature 25 °C, flow rate 1.0 mL/min. UV detection at 210 nm.

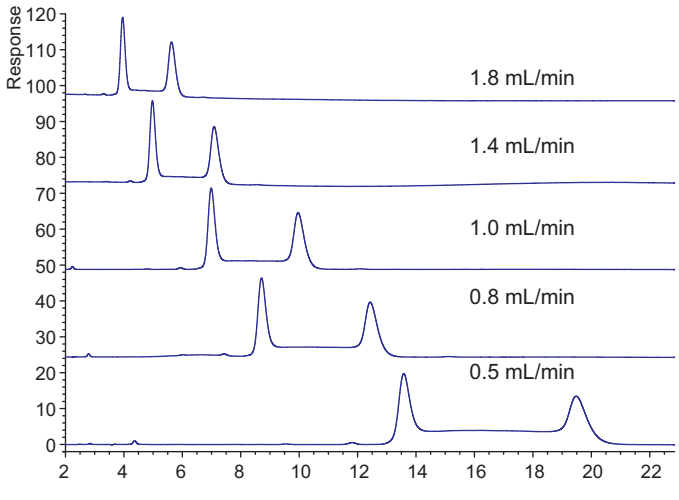

Fig. 6. Influence of the flow-rate variation on the on-column interconversion of triphenyl atropisomers. Chromatographic conditions: Obelisc R (4.6 × 150 mm), water (0.1 vol.% H_3PO_4)–acetonitrile (60/40, v/v) mobile phase, column temperature 25 °C, UV detection at 210 nm.

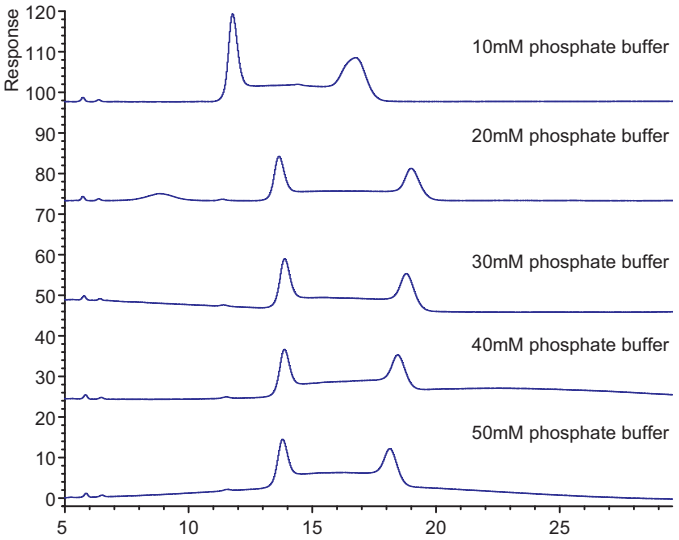

Fig. 7. Influence of ionic strength on the on-column interconversion of triphenyl atropisomers. Chromatographic conditions: Obelisc R (4.6 × 150 mm), water (phosphate buffer, pH 2.2)–acetonitrile (60/40, v/v) mobile phase, column temperature 25 °C, UV detection at 210 nm.

be inferred from analysis of the elution profiles, initial increase of buffer concentration from 10 to 30 mM (at a constant pH of 2.2) resulted in a minor increase in retention time for both pure components, which was accompanied by a small increase in the plateau area between the peaks. The observed effect might be associated with increased ionic strength of the mobile phase eluent, which potentially can enhance hydrophobic interactions due to suppression of charge interactions resulting in longer retention and decreased rate of chromatographic separation. Regardless, the latter effect appears to be weak; increase of buffer concentration beyond 30 mM produced no detectable changes in the conformers' retention or affected their corresponding peak areas.

3.2. Stereodynamic analysis of atropisomer separation

3.2.1. Analysis of dynamic HPLC data

Dynamic HPLC is well suited for kinetic analysis of interconversion. A *de rigueur* requirement for application of this technique is on-column separation of interconverting isomers. As noted above, chromatographically this phenomenon is revealed as plateau formation between two peaks, peak broadening and eventually peak coalescence. The elution profiles of interconverting species are manifestations of the interconversion rate constant and timescale of chromatographic separations, and as such can be used to extract kinetic information. Additionally, thermodynamic information can be extracted from retention analysis of unconverted component peaks (as will be discussed in Section 3.2.2).

The rate constants and activation energy barriers determined from dynamic chromatography data represent apparent values of these parameters, since with this method it is not possible to differentiate between the rates constants in the mobile phase and stationary phase. Additional data from second technique are needed to independently assess the interconversion rate in the mobile phase. Both surface phenomena and given experimental conditions (temperature inside column, thermal gradients, etc.) can influence the interconversion rate. In general these effects are rather small [12], but for selected systems stationary phase reportedly increased isomerization barrier by 1.0–5.5 kJ/mol [17,18]. Thus, experimentally determined rate constants are weighed averages of rate constants of different interconversion processes taking place in the mobile and stationary phases, and as such should be referred to as "apparent".

Methods for evaluation of the interconversion rate constants in chromatographic processes are based on several theoretical models, such as the theoretical plate model, stochastic model, continuous flow model as well as a number of semi-empirical approaches and approximation functions. Reviews of the dynamic chromatography methods and calculation approaches can be found in several literature sources [19–21].

The interconversion of a molecule containing a stereo labile fragment can be described by the following equilibrium:

$$a \underset{k_{-1}}{\overset{k_1}{\rightleftharpoons}} b$$

In the above reaction a and b represent interconverting isomers of a molecule in the given study, and k_1 and k_{-1} are the rate constants of the forward ($a \rightarrow b$) and reverse ($b \rightarrow a$) interconversion reactions. The atropisomerization process typically constitutes a reversible first order reaction. However, in the process of dynamic chromatography the interconverting isomers are physically separated, and assumed not to significantly interfere with each other during migration through the column. As shown by several authors, for dynamic chromatography the apparent rate constants can be described by the following rate equations derived for irreversible first order reactions [5,21]:

$$k_1 = \frac{1}{t_{R,A}} \ln \frac{[a]_0}{[a]} \tag{1}$$

$$k_{-1} = \frac{1}{t_{R,B}} \ln \frac{[b]_0}{[b]} \tag{1a}$$

where t_R is the retention time, while $[a]$ and $[b]$ are the concentrations (or area counts) of the non-interconverted isomers, subscript zero denotes the initial concentration (i.e. prior to interconversion at time $t = 0$). The temperature dependence of the rate constants are described by the well-known Arrhenius equation:

$$\ln k_1 = -\frac{E_a}{RT} + \ln A_1 \tag{2}$$

$$\ln k_{-1} = -\frac{E_a}{RT} + \ln A_{-1} \tag{2a}$$

where E_a is the activation energy, R is the universal gas constant, T is the absolute temperature, and A_1 (or A_{-1}) is the pre-exponential constant. As can be inferred from the above equation, if the reaction rate obeys Arrhenius equation the plot of $\ln k$ as a function of reciprocal temperature ($1/T$) should be linear with the slope and intercept providing information about the magnitude of the activation energy and pre-exponential factor, respectively.

Similarly, from the Transition State Theory, the Gibbs free energy of activation for the process can be calculated using the Eyring equation [22]:

$$k_1 = \kappa \frac{k_B T}{h} \exp\left(-\frac{\Delta G^{\neq}}{RT}\right) \tag{3}$$

$$k_{-1} = \kappa \frac{k_B T}{h} \exp\left(-\frac{\Delta G^{\neq}}{RT}\right) \tag{3a}$$

where κ is the transmission coefficient (usually taken to be unity), k_B is the Boltzmann's constant, h is the Planck's constant, and $\Delta G^{\neq}$ is the apparent energy of activation for the process. Expressing the Gibbs energy as

$$\Delta G^{\neq} = \Delta H^{\neq} - T\Delta S^{\neq} \tag{4}$$

and making appropriate rearrangements, the linear form of the Eyring equation can be obtained:

$$\ln\left(\frac{k_{1,-1}}{T}\right) = -\frac{\Delta H^{\neq}}{R}\frac{1}{T} + \ln\left(\frac{k_B}{h}\right) + \frac{\Delta S^{\neq}}{R} \tag{5}$$

By plotting the $\ln(k/T)$ dependence on $(1/T)$ the enthalpy of activation can be determined from the slope of this plot ($-\Delta H^{\neq}/R$), while the entropy of activation can be calculated from the intercept ($\ln(k_B/T) + \Delta S^{\neq}/R$).

For a given system both Arrhenius and Eyring equations are expressions of the same apparent rate constant and the right sides of these equations can be equated. After simple mathematical operation it can be shown that for reactions in solution

$$E_a = \Delta H^{\neq} + RT \tag{6}$$

Since activation energy is related to the Gibbs free energy of activation, it contains both enthalpic and entropic contributions.

The results of kinetic analysis of temperature dependent "reaction chromatograms" are summarized in Tables 1 and 2. First eluting isomer is denoted by letter "*a*", and the second by letter "*b*". Peak areas at 5 °C (278 K) were not affected by interconversion, so these respective peak areas were used for initial concentration of each interconverting isomer ($t = 0$). Temperature-dependent rate constants were obtained using Eq. (1), where $[a]$ and $[b]$ values were obtained through deconvolution of the reaction chromatograms using standard integration functions in Atlas 8.2 (Thermo Electron Corp.) software. As can be noticed, the rate constants of both

Table 1
Kinetic and thermodynamic parameters for $a \rightarrow b$ interconversion ("forward" reaction). *Note*: first eluting isomer is denoted by letter "*a*".

T (K)	t (s)	[a] (counts)	$k_{app}^{a\rightarrow b}$ (s^{-1})	$\Delta G^{\#}$ (kJ/mol)	$-T\Delta S^{\neq a\rightarrow b}$ (kJ/mol)
278		1098	–	–	–
283	484	1058	0.000076	89.9	−9.9
288	476	1031	0.000130	90.2	−10.1
293	460	950	0.000314	89.7	−10.2
298	445	816	0.000666	89.4	−10.4
303	425	639	0.001271	89.3	−10.6
308	406	419	0.002372	89.2	−10.8
313	386	159	0.005013	88.8	−10.9

Standard errors for ($\Delta G^{\#}$) and ($T\Delta S^{\neq}$) were estimated to be ±3.0 and ±2.0 kJ/mol, respectively.

Table 2
Kinetic and thermodynamic parameters for $b \rightarrow a$ interconversion ("reverse" reaction). *Note*: first eluting isomer is denoted by letter "*a*".

T (K)	t (s)	[b] (counts)	$k_{app}^{b\rightarrow a}$ (s^{-1})	$\Delta G^{\#}$ (kJ/mol)	$-T\Delta S^{\neq b\rightarrow a}$ (kJ/mol)
278		1081			
283	759	1063	0.000023	94.3	−23.8
288	727	1034	0.000062	93.6	−24.2
293	683	973	0.000155	93.1	−24.6
298	643	887	0.000308	93.0	−25.0
303	598	719	0.000683	92.6	−25.5
308	551	471	0.001509	92.2	−25.9
313	499	195	0.003433	91.5	−26.3

Standard errors for ($\Delta G^{\#}$) and ($T\Delta S^{\neq}$) were estimated to be ±2.5 and ±1.8 kJ/mol, respectively.

forward and reverse processes are strongly influenced by the temperature, and the rate of either interconversion reaction nearly doubles for each ten degree increase in temperature. For all temperatures in the range studied the rate of the forward reaction ($a \rightarrow b$) is always higher then that of the reverse. However, this difference becomes less pronounced as the temperature in chromatographic system increases from 5 °C (283 K) to 40 °C (313 K).

Linear form of Arrhenius equation (equation (2)) was used to extract information about activation energies of the $a \rightarrow b$ and $b \rightarrow a$ interconversion processes. Goodness of fit for linear regression data as determined by r^2 (squared correlation coefficient) was 0.998, or higher. The corresponding data plots are shown in Fig. 8. The values of activation energies for the forward and reverse interconversion reactions were 104.0 ± 2.3 kJ/mol and 120.4 ± 1.9 kJ/mol, respectively. The activation energies determined in this study were consistent with results reported for other structures containing single biphenyl fragment [23].

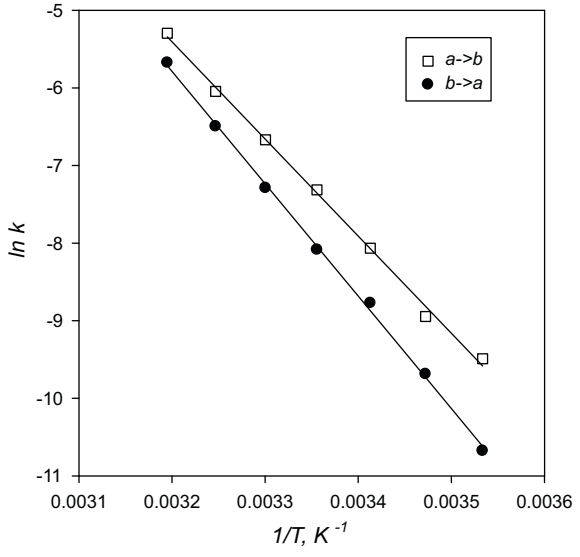

Fig. 8. Arrhenius plots for forward and reverse interconversion reactions. First eluting isomer is denoted by letter "*a*".

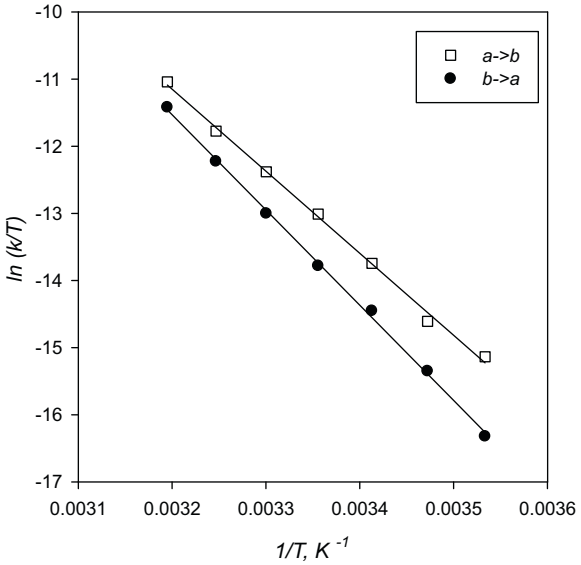

Fig. 9. Eyring plots for the forward and reverse interconversion reactions. First eluting isomer is denoted by letter "*a*".

Additionally, activation energy values were estimated from flow rate-dependent and pH-dependent "reaction chromatograms". For the flow rate study the averaged activation energy values were determined to be 106.0 ± 2.3 and 122.8 ± 2.0 kJ/mol for the forward and reversed interconversion reactions. For pH studies the activation energy values were 105.7 ± 2.5 and 123.0 ± 2.4 kJ/mol, respectively. The values of the activation energy obtained in these studies are essentially equivalent within experimental error, which indicated that solvent effects had insignificant impact on energetics of activation for the interconversion process.

Although the activation energy determined from the Arrhenius equation is widely reported in kinetic studies, the Eyring equation has the advantage of allowing independent calculation of the enthalpy and the entropy of activation. To gain better understanding of the interconversion process, the experimentally determined temperature dependent rate data were analyzed using linear form Eyring Eq. (5). The corresponding plots are shown in Fig. 9. Both forward and reverse reaction plots exhibited good linearity with r^2 coefficient of 0.998 or higher. Slope values of these plots were used to calculate enthalpies of activation process. For the forward reaction enthalpy of activation $\Delta H^{\neq}$ was determined to be 101.6 ± 2.3 kJ/mol, and for the reverse reaction 117.9 ± 2.0 kJ/mol. Using Eq. (6) one can easily show that these data are in good agreement with activation energies obtained from Arrhenius equation.

The intercept values of the Eyring plots were used to calculate the apparent entropy of activation process. For the forward reaction $\Delta S^{\neq}$ value of 35 ± 7 JK^{-1} mol^{-1} was obtained, and for the reverse process 84 ± 6 JK^{-1} mol^{-1}. Although both reaction processes reveal small positive values of the entropic term, the reverse $b \rightarrow a$ process exhibits significantly larger contribution of temperature–entropy product to the apparent Gibbs free energy of activation (Tables 1 and 2). These numbers being statistically different pinpoint towards the differences in the sterical hindrance of rotation exhibited by interconverting species in transition state. Overall, the magnitude of entropy values (resulting from rotational motion) appears to be consistent with other data reported in literature [5,24].

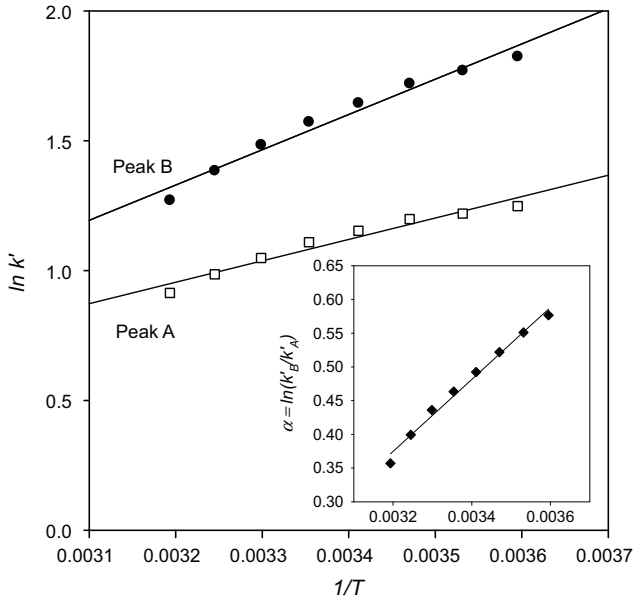

Fig. 10. Influence of temperature on retention and selectivity of the triphenyl separation.

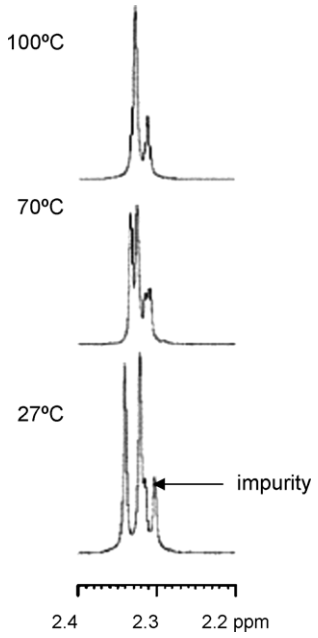

Fig. 11. Temperature-dependent ^{1}H NMR spectra of the methyl group attached to the terminal aromatic ring of triphenyl. Please note that the spectrum shown also contains two low intensity peaks resulting from the presence of a known, structurally-related impurity.

As an alternative to the approach taken in this work, one might consider treating fewer reaction chromatograms with more sophisticated software in order to obtain an assessment of the activation parameters [25,26]. The authors chose instead to treat larger experimental data sets, in a simple manner, to obviate any potential ambiguity in the results that might come in from various errors introduced via more complex modeling efforts. More importantly, "experimentally-heavy" approach to dynamic chromatography utilized herein allowed for the simultaneous optimization of chromatographic parameters (during method development) required for routine separation of process intermediates and impurities (not discussed in the current paper).

3.2.2. Thermodynamic analysis of retention data

To supplement kinetic analysis presented above, additional information on driving forces of the triphenyl atropisomers retention and selectivity mechanism can be obtained from thermodynamic analysis of retention data. The van't Hoff plots [27] constructed for isomers *a* and *b* using temperature-dependent retention data are shown in Fig. 10. The plots of retention data exhibited linear fit correlation coefficient r^2 of 0.955 or higher. Although adequately linear, somewhat lower then expected values of correlation coefficient might be attributed to uncertainty of retention time determination at higher temperatures, i.e. when peaks of individual atropisomers begin to significantly co-elute (coalesce). Linear form of van't Hoff plots indicated that stationary phase did not undergo any conformational changes in the temperature range studied. As a general trend individual retention plots showed decrease of retention time with increase in temperature. For both isomers van't Hoff plots exhibited positive slope indicative of enthalpy driven retention process (slope = $-\Delta H^\circ/R$).

The selectivity factor is a quantity that represents a difference in the free energy of interaction of the two isomers with the stationary phase, i.e. $\ln\alpha = -\Delta\Delta G^\circ/RT = -(\Delta\Delta H^\circ/RT) + (\Delta\Delta S^\circ/R)$ [25]. Thus, for a given system the plot of logarithmic selectivity as a function of reciprocal temperature yields valuable information on driving forces of chromatographic separation. The results of this analysis are shown in the insert of Fig. 10. The selectivity plot for atropisomers *a* and *b* was linear with a correlation coefficient of 0.989, indicating that selectivity mechanism did not change over the temperature range studied. From the slope and the intercept the differences in standard enthalpy and entropy were determined to be $\Delta\Delta H^\circ = -4.4 \pm 0.2$ kJ/mol and $\Delta\Delta S^\circ = -11 \pm 0.8\,\mathrm{J\,K^{-1}\,mol^{-1}}$. Thus, thermodynamic data revealed that chromatographic selectivity of the triphenyl isomers separation process was driven primarily by enthalpy dominated mechanism throughout the entire temperature range. Finally, it should be mentioned that thermodynamic parameters determined in the study are analyte-structure and system dependent.

3.2.3. Dynamic NMR study

In order to determine the activation parameters of atropisomer interconversion, ^{1}H NMR experiments were initially planned to be performed in deuterated acetonitrile–D_2O diluent to closely mimic chromatographic system. However, triphenyl sample had poor solubility in these solvents so that suitable spectra could not be obtained. As a result all variable temperature ^{1}H NMR experiments were recorded in deuterated dimethylsulfoxide. The resonance signals of the methyl group (Fig. 2) attached to the terminal aromatic ring, distinctly separated from other peaks in the spectrum, was used for data analysis. The temperature dependent changes of the methyl group chemical shift are shown in Fig. 11 (please note that the spectrum shown also contains two low intensity peaks resulting from the presence of a known, structurally-related impurity). At room temperature the resonance signals of the methyl group protons appear as a doublet (peaks located at 2.32 ppm and 2.34 ppm, see Fig. 11) resulting from two magnetically nonequivalent orientations of methyl in atropisomers. As the temperature was increased, the resonance signals were observed to shift, eventually merging into a single peak. This is an indication that upon reaching the coalescence temperature the interconversion process is faster than the spin-lattice relaxation. From the variable temperature ^{1}H NMR experiments the coalescence temperature (T_C) was determined to be 373 K.

At the coalescence temperature the rates of the forward and reverse interconversion reactions become equal, and the rate of interconversion reaction can be expressed by the following equa-

tion [28]:

$$k_C = k_1 = k_{-1} = \frac{\pi}{\sqrt{2}} \left|\Delta\nu\right| \quad (7)$$

where $\Delta\nu$ is the chemical shift difference. Thus, at the coalescence temperature $\Delta G^{\neq}$ can be expressed as follows:

$$\Delta G^{\neq} = RT_C \ln \frac{RT_C}{k_C N_A h} \quad (8)$$

where N_A is Avogadro's number, and T_C is the coalescence temperature. At 373 K the interconversion rate constant was determined to be $8\,s^{-1}$, and the free energy of the activation process at the coalescence temperature was calculated to be 85.6 ± 2.4 kJ/mol.

For comparison purposes, the free energy of activation at T_C can be estimated from $(\Delta H^{\neq} - T\Delta S^{\neq})$ relationship using the dynamic chromatography data. For the forward and reverse interconversion processes the $\Delta G^{\neq}_{(373\,K)}$ values of 88.6 ± 3.0 kJ/mol and 86.6 ± 2.5 kJ/mol, respectively, were obtained extrapolating lower temperature dynamic chromatography data to 373 K. Taking into consideration the experimental errors, the apparent values obtained from dynamic chromatography are in a good agreement with the free energy values obtained from NMR. The stationary phase and solvent appear to have minor effect to the overall energetics of interconversion process, and their contributions cannot be clearly distinguished within the margin of error of the techniques employed in the study.

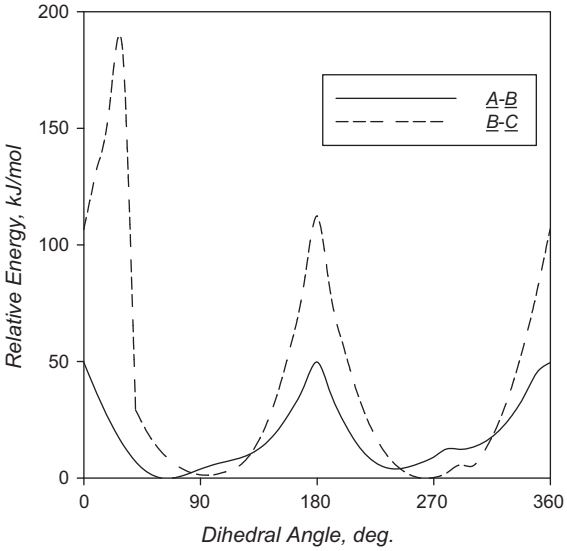

Fig. 12. Conformer relative energy as a function of dihedral angle formed by the planes of the phenyl rings *A*, *B* and *C*. For the rings designations in the molecular structure refer to Fig. 2.

4. Computational studies

Restricted rotation in the TP molecule is of particular interest, as this molecule contains three phenyl rings while most of the literature data on dynamic chromatography primarily deals with simple biphenyls [29,30]. Thus, as can be inferred from the molecular structure, existence of the triphenyl rotamers may be a result of restricted rotation along the single bond connecting the aromatic rings *A*–*B*, or *B*–*C* (Fig. 2).

In the latter case, the internal phenyl rings *B* and *C* both have *ortho*-substituents. For simple biphenyls, literature data indicate that such systems studied by dynamic LC typically exhibit activation energies in the range of 70–120 kJ/mol [11,12], and the energy barriers are correlated with the size of *ortho*-substitutents [23]. However, for a complex triphenyl molecule internal *B*–*C* rotation might be too restrictive (as compared to simple biphenyls) as a result of sterical hindrance caused by bulky long tail substituent present on the ring *C*. In that case, the experimentally observed interconversion phenomenon might be attributed to the *A*–*B* bond, where rotation speed might be impacted by the presence of electron-withdrawing carboxyl group in the *para*-position with respect to the *A*–*B* bond [24].

In order to gain insight into the conformational changes taking place during interconversion process, molecular modeling studies for the triphenyl molecules were undertaken. At first the triphenyl structure was minimized to obtain the lowest energy conformer (global minimum) using molecular mechanics force field (MMFF). Subsequently, the transition state species was modeled as the highest-energy configuration that could be obtained via bond-rotation connecting each of the phenyl rings of interest. Energy profile for rotational conformers was generated using MMFF method.

Fig. 12 shows relative energy of conformers as a function of dihedral angle formed by rotation of the respective pairs of phenyl rings. For the dihedral rotation *A*–*B*, there are two maxima at 0° and 180° which correspond to a coplanar orientation of the phenyl rings. Both maxima are of equal energy (50 kJ/mol.), suggesting that either in-plane orientation of rings *A* and *B* presents essentially the same energy barrier (same sterical hindrance) to overcome for rotation about this bond. Contrastingly, for dihedral rotation about *B*–*C* there are two distinct maxima. The maximum at 30° corresponds to a position of highest overlap of the chloro- and methamine tail *ortho*-substituents (pertaining to *B*–*C* rings). The other maximum at 180° corresponds to coplanar ring orientation when those two *ortho*-groups are facing in the opposite direction.

From the energetic perspective, transition state resulting from dihedral rotation *B*–*C* has an estimated activation energy barrier of 112 kJ/mol. Although this number is twice as high as the activation barrier for *A*–*B* rotation, it is still well within the range of activation energy values measured by dynamic HPLC. On the other hand, 50 kJ/mol computed for *A*–*B* rotation is rather low to be experimentally observed in dynamic LC experiment (i.e. rate of interconversion is fast relative to rate of isomer separation). It is also worth noting that the energy difference between ground state conformers for *B*–*C* rotation is under 0.3 kJ/mol suggesting that both energy states are nearly equally populated. This result is supported experimentally by the dynamic chromatography studies which consistently showed equal size peaks of the interconverting species (in cases where there was separation).

Additional model verification was performed with Hartree-Fock method using 6-31* base set. To save computational time, energy profile calculations were conducted for a simple triphenyl molecule, where a side chain on the ring *C* was truncated at the amine group (not shown). The activation energy values computed using higher level of theory were within ten percent agreement with results obtained using molecular mechanics method.

Thus, the modeling studies support a conclusion that restricted rotation of the *B*–*C* single bond gives rise to atropisomer formation. Simulation of the dihedral rotation indicates that the bulky *ortho* substituent on ring *C* does not present impassable barrier to rotation about *B*–*C* bond due to great conformational flexibility of methylamine substituent chain. The determined activation energy value of 112 kJ/mol is in a reasonable agreement with experimentally measured apparent activation energy values obtained from dynamic chromatography (see Arrhenius data). Some discrepancy in the estimated values can be attributed to computational study being performed in the vacuum, as both stationary phase and mobile phase solvents can impact activation energy in transition state.

5. Summary and conclusions

The pharmaceutical triphenyl molecule contains three stereogenic elements: two chiral centers and one chiral axis at the *B–C* rings. Rotation of the single bond between the *A–B* rings has a much lower energy barrier, therefore it does not effectively form a stereogenic element. The atropisomers observed in the study are due to restricted (higher energy) rotation of the single bond connecting the *B–C* rings. Separation of pharmaceutical triphenyl configurational isomers, challenging to accomplish using more traditional phases, was readily performed over a conventional temperature range using Obelisc R, a novel mixed mode stationary phase. The underlying mechanism of separation appears to be driven by both hydrophobic and simultaneous charge interactions. Molecular modeling and variable temperature NMR studies suggested that restricted rotation along a single biphenyl bond was responsible for the atropisomerism.

Reaction chromatograms of isomer interconversion observed in the study were consistent with first order kinetics. From the analysis of dynamic chromatography data activation energy of the exchange process (E_a) was determined to be 104.0 ± 2.3 kJ/mol and 120.4 ± 1.9 kJ/mol for the forward and reverse interconversion reactions, respectively. A similar value (112 kJ/mol) was obtained from molecular modeling calculations in vacuum. Activation energy values obtained in the study were in good agreement with the values for biphenyl systems reported in literature, where there are *ortho* substituents on each of the rings.

Treatment of dynamic chromatography data was complimented with the Eyring equation analysis to assess the enthalpy, and entropy of activation. Calculation of the Gibbs free energy of activation process at coalescence temperature extrapolated from lower temperature dynamic chromatography data was in good agreement with direct measurement of $\Delta G^{\neq}$ at coalescence temperature obtained from variable temperature NMR experiments (88.6 ± 3.0 kJ/mol and 86.6 ± 2.5 kJ/mol for forward and reverse processes from dynamic HPLC vs. 85.6 ± 2.4 kJ/mol from NMR). These findings indicate that stationary phase and solvent effects had insignificant effect on intra-molecular motion occurring through single bond rotation. The above study also underscores complementing nature of dynamic HPLC and NMR techniques which can be used to supplement each other in kinetic studies of atropisomerism of biphenyl containing compounds.

From thermodynamic perspective, the underlying mechanism of atropisomer separation was dominated by enthalpic interactions arising from a combination of both hydrophobic and charge interactions. Overall, separation of triphenyl atropisomers demonstrates the utility of novel mixed mode Obelisc R phase for challenging analytical problems.

Acknowledgements

Authors acknowledge Drs. Edward Sherer, Vincent Antonucci, and Chris Welch for helpful discussions during the manuscript preparation.

References

[1] B. Liberek, J. Augustyniak, J. Ciarkowski, K. Plucinska, K. Stachowiak, J. Chromatogr. 95 (1974) 221.
[2] O. Trapp, G. Schoetz, V. Schurig, Chirality 3 (2001) 403.
[3] J. Krupcik, P. Oswald, P. Majek, P. Sandra, D. Armstrong, J. Chromatogr. A 1000 (2003) 779.
[4] P. Oswald, K. Desmet, P. Sandra, J. Krupcik, D.W. Armstrong, Chirality 14 (2002) 334.
[5] J. Krupcik, J. Mydlova, P. Majek, P. Simon, D.W. Armstrong, J. Chromatogr. A 1186 (2008) 144.
[6] S. Reich, O. Trapp, V. Schurig, J. Chromatogr. A 892 (2000) 487.
[7] P. Osswald, F. Wurthner, JACS 129 (2007) 14319.
[8] M. Carrozzo, G. Cannazza, U. Battisti, D. Braghiroli, C. Parenti, Chirality 22 (2010) 389.
[9] A. Fedurcova, M. Vancova, J. Mydlova, J. Lehotay, J. Krupcik, J. Chromatogr. Relat. Technol. 29 (2006) 2889.
[10] I. D'Acquarica, F. Gasparrini, D. Kotoni, M. Pierini, C. Villani, W. Cabri, Molecules 15 (2010) 1309.
[11] G. Shoetz, O. Trapp, V. Schurig, Enantiomer 5 (2000) 391.
[12] I. D'Acquarica, F. Gasparini, M. Pierini, C. Villani, G. Zappia, J. Sep. Soc. 29 (2006) 1508.
[13] C. Wolf, G. Tumambac, J. Phys. Chem. A 107 (2003) 815.
[14] Obelisc Brochure by SIELC Technologies, http://www.sielc.com.
[15] Y. Zelechonok, SIELC, private communication.
[16] M. Lammerhofer, M. Richter, J. Wu, R. Nogueira, W. Bicker, W. Lindner, J. Sep. Sci. 31 (2008) 2572.
[17] F. Gasparini, D. Misti, M. Pierini, Tetrahedron: Asymmetry 8 (1997) 2069.
[18] J. Oxelbark, S. Allenmark, J. Chem. Soc., Perkin Trans. 2 (1999) 1587.
[19] O. Trapp, G. Schoetz, V. Schurig, Chirality 13 (2001) 403.
[20] O. Trapp, Chirality (2006) 489.
[21] P.J. Skrdla, V. Antonucci, C. Lindemann, J. Chromatogr. Sci. 39 (2001) 431.
[22] P.W. Atkins, Physical Chemistry, Oxford University Press, Oxford, 1998.
[23] C. Wolf, H. Xu, Tetrahedron Lett. 48 (2007) 6886.
[24] M.I. Page, The Chemistry of Enzyme Action, Elsevier, 1984, p. 20.
[25] O. Trapp, Anal. Chem. 78 (2006) 189.
[26] L. Pasti, A. Cavazzini, M. Nassi, F. Dondi, J. Chromatogr A 1217 (2010) 1000.
[27] Cs. Horvath, W.R. Melander, in: E. Heftmann (Ed.), Chromatography, Fundamentals and Applications of Chromatographic and Electrophoretic Methods, Elsevier, New York, 1983, p. A28.
[28] J. Sandstrom, Dynamic NMR Spectroscopy, Academic Press, New York, 1982.
[29] C. Wolf, D. Hochmuth, W. Konig, C. Roussel, Liebigs Ann. Chem. 3 (1996) 357.
[30] C. Wolf, Chem. Soc. Rev. 34 (2005) 595.